Available online at www.sciencedirect.com
ScienceDirect
Agricultural and Forest Meteorology 147 (2007) 125–139
AGRICULTURAL AND FOREST METEOROLOGY
www.elsevier.com/locate/agrformet

Air and biomass heat storage fluxes in a forest canopy: Calculation within a soil vegetation atmosphere transfer model

Vanessa Haverd [a,c,*], Matthias Cuntz [b,1], Ray Leuning [c], Heather Keith [d]

[a] Department of Chemistry, University of Wollongong, NSW 2522, Australia
[b] Research School of Biological Sciences, GPO Box 475, Canberra, ACT 2601, Australia
[c] CSIRO Marine and Atmospheric Research, GPO Box 3023, Canberra, ACT 2601, Australia
[d] CSIRO Climate Program, GPO Box 3023, Canberra, ACT 2601, Australia

Received 19 October 2006; received in revised form 4 June 2007; accepted 19 July 2007

Abstract

An analytical method for calculating the sub-diurnal change in heat storage in tree trunks is presented and incorporated in a soil vegetation atmosphere transfer (SVAT) model. The modelled change in biomass heat storage (J_{tr}) is driven by radial heat diffusion within the trunks and surface heat exchange by convection, insolation and longwave radiation. The calculation requires only variables from the previous and current time step and is independent of measured biomass temperature. The model was applied to a 40 m tall Australian temperate Eucalyptus forest at the Tumbarumba Ozflux site. A comparison between modelled and measured trunk temperatures showed agreement to within 1 °C, providing confidence in the model. Hourly values of J_{tr} peaked at 61 W m^{-2} for this site. Similar values of J_{tr} were obtained using an adaptation of the force-restore method. Additional calculations for a range of leaf area indices and trunk radii enable a quick estimate of the maximum hourly value of J_{tr} for any forest with given leaf area index, quadratic mean trunk radius (at breast height) and biomass. Inclusion of heat storage fluxes in the hourly available energy budget for the forest improved agreement between available energy and measured heat fluxes above the canopy, with energy closure rising from 90 to 101%. Accounting for J_{tr} in the SVAT model also improved agreement between measured and modelled fluxes of sensible and latent heat.

Keywords: Biomass heat storage; Energy closure; SVAT model; Forest

1. Introduction

The rate of change of canopy energy storage (or energy storage flux), J_c, can be a significant component of the sub-diurnal surface energy budget in a tall forest, owing to the large volumes of air and biomass in the canopy. For example, Moore and Fisch (1986) reported maximum absolute hourly canopy storage fluxes of around 80 W m^{-2} for a 35 m tall Amazonian tropical forest and Silberstein et al. (2001) obtained similar values for a 30 m tall *Eucalyptus marginata* forest in Western Australia. In such cases, the heat storage flux is a significant component of the net radiation absorbed by the canopy and soil. Thus it is expected that accounting for J_c in the available energy budget should significantly affect energy closure, i.e. the slope of the regression line relating turbulent energy fluxes measured above the canopy to the available energy. If J_c is significant, it should also be computed in any soil vegetation atmosphere transfer (SVAT) model that attempts to partition available energy between canopy and soil, and

* Corresponding author at: CSIRO Marine and Atmospheric Research, GPO Box 3023, Canberra, ACT 2601, Australia.
Tel.: +61 2 6246 5981; fax: +61 2 6246 5988.
E-mail address: vanessa.haverd@csiro.au (V. Haverd).
[1] Now at: Max-Planck-Institut für Biogeochemie, Hans-Knöll-str. 10, 07745 Jena, Germany.

0168-1923/$ – see front matter
doi:10.1016/j.agrformet.2007.07.006

Nomenclature

A	trunk surface area (m^2 (trunk) m^{-2} (ground))
B_n	coefficient in solution to heat diffusion equation in cylindrical co-ordinates (Eq. (12))
$B^*_{net,tr}$	net isothermal longwave radiation absorption by trunks (W m^{-2} (trunk))
$B_{net,tr}$	net longwave radiation absorption by trunks (W m^{-2} (trunk))
c_l	specific heat capacity of leaves (J kg^{-1} K^{-1})
c_p	specific heat capacity of air (J kg^{-1} K^{-1})
c_s	specific heat capacity of soil (J kg^{-1} K^{-1})
C_s	volumetric heat capacity of soil (J kg^{-1} K^{-1})
c_{tr}	specific heat capacity of trunks (J kg^{-1} K^{-1})
d_{bh}	trunk diameter at breast height (1.3 m) (m)
D_h	thermal diffusivity of air (m^2 s^{-1})
F_{CO_2}	net CO_2 flux out of canopy (mg CO_2 m^{-2})
G	heat flux into the soil (W m^{-2} (ground))
h	surface conductance (convective plus radiative) (W m^{-2} K^{-1})
h_c	surface conductance (convective) (W m^{-2} K^{-1})
h_r	surface conductance (radiative) (W m^{-2} K^{-1})
H_{tr}	sensible heat flux away from trunk surface (W m^{-2} (ground))
J_a	change in sensible heat storage in the air (W m^{-2} (ground))
J_c	change in heat storage in the canopy (W m^{-2} (ground))
J_l	change in sensible heat storage in the leaves (W m^{-2} (ground))
J_p	rate of energy storage by photosynthesis (W m^{-2} (ground))
J_{tr}	change in sensible heat storage above-ground woody biomass (W m^{-2} (ground))
J_w	change in latent heat storage in the air (W m^{-2} (ground))
k	thermal conductivity (W m^{-1} K^{-1})
m_{tr}	mass of above-ground (wet) woody biomass (kg m^{-2} (ground))
n_{tr}	number density of trees (m^{-2} (ground))
q	surface energy flux (W)
r	perpendicular distance from trunk axis (m)
R	trunk radius (m)
$\overline{R}(z)$	quadratic mean trunk radius at height z (m)
$\overline{R}_{bh}$	quadratic mean trunk radius at 1.3 m (m)
$R^*_{net,tr}$	net isothermal radiation absorption by trunks (W m^{-2} (trunk))
$S_{net,tr}$	net solar radiation absorption by trunks (W m^{-2} (trunk))
t	time (s)
T_a	air temperature (K)
T_{soil}	soil surface temperature (K)
T_{tr}	trunk temperature (K)
$T_{tr,S}$	trunk surface temperature (K)
u	wind speed (m s^{-1})
z	height above forest floor (m)

Greek letters

Λ	total vegetation area index (m^2 (vegetation) m^{-2} (ground))
Λ_L	total leaf area index (m^2 (leaf) m^{-2} (ground))
Λ_{tr}	total trunk area index (m^2 (trunk) m^{-2} (ground))
α_{tr}	reflectance of trunk surface
α_L	leaf reflectance
α_{soil}	soil reflectance
χ_w	mixing ratio of water vapour in dry air kg (H_2O) kg^{-1} (dry air)
ε_{air}	sky emissivity
ε_{soil}	soil emissivity
ε_{tr}	trunk emissivity
κ	thermal diffusivity (m^2 s^{-1})
λ	latent heat of vaporisation (J kg^{-1})
λ_n	root of transcendental (Eq. (13))
ν	kinematic viscosity of air (m^2 s^{-1})
θ	temperature difference ($T_{tr} - T_a$) (K)
ρ	density of moist air (kg m^{-3})
ρ_d	density of dry air (kg m^{-3})
ρ_l	density of leaves (per m^3 canopy volume) (kg m^{-3})
ρ_{tr}	specific density of trunks (kg m^{-3})
$\rho_{tr,d}$	density of dry wood in trunks (kg m^{-3})
σ	Stefan–Boltzmann constant (W m^{-2} K^{-4})
τ	diurnal period (s)
ω	vegetation scattering coefficient
ξ	cumulative vegetation area (m^2 (vegetation) m^{-2} (ground))
ξ_L	cumulative leaf area (m^2 (leaf) m^{-2} (ground))
ξ_{tr}	cumulative vegetation area (m^2 (vegetation) m^{-2} (ground))

between sensible and latent heat fluxes on a sub-diurnal time scale. The rate of change of energy storage in the canopy is the sum of several components:

$$J_c = J_a + J_w + J_l + J_{tr} + J_p \tag{1}$$

where J_a, and J_w are the sensible and latent heat storage fluxes in the air column below the flux measurement height, z_r, above the canopy. J_l and J_{tr} are the heat storage fluxes in the leaves and above-ground woody biomass respectively and J_p is the rate of energy storage by photosynthesis. The storage fluxes in the air column,

$$J_a = \int_0^{z_r} \rho c_p \frac{dT_a}{dt} dz \cong \rho c_p \sum_{i=1}^{n} \left(\frac{\Delta T_a}{\Delta t} \Delta z_i \right) \tag{2}$$

$$J_w = \int_0^{z_r} \rho_d \lambda \frac{d\chi_w}{dt} dz \cong \rho_d \lambda \sum_{i=1}^{n} \frac{\Delta \chi_w}{\Delta t} \Delta z_i \tag{3}$$

are readily estimated from vertical profiles of temperature and vapour pressure (see Nomenclature). In Eqs. (2) and (3), the sums are over all measurement heights, Δz_i is the difference between successive measurement heights, and Δt is the difference in time between successive measured profiles. Similarly the storage flux in leaves:

$$J_l = \int_0^{z_r} \rho_l c_l \frac{dT_l}{dt} dz \cong \rho_l c_l \sum_{i=1}^{n} \left(\frac{\Delta T_{l,i}}{\Delta t} \Delta z_i \right) \tag{4}$$

is readily estimated from leaf temperatures or, in their absence, $\Delta T_{a,i}$, can be substituted for $\Delta T_{l,i}$ (Blanken et al., 1997). J_p is typically estimated as the net CO_2 uptake, $-F_{CO_2}$, multiplied by a photosynthetic conversion factor of $C = 0.469$ J μmol^{-1} (Blanken et al., 1997).

The heat storage flux in the above-ground woody biomass (trunks and branches) can be expressed as:

$$J_{tr} = \int_0^{h_c} m_{tr} c_{tr} \frac{d\left\langle T_{tr}(z) \right\rangle}{dt} dz \tag{5}$$

where $\langle T_{tr}(z) \rangle$ is some spatially averaged biomass temperature, m_{tr} is the mass of trunks and branches per unit of horizontal area and c_{tr} is the specific heat capacity of the trunks and branches. J_{tr} is the least easily estimated component of Eq. (1).

Attempts to date to include J_{tr} in the canopy energy budget have mostly relied on temperature measurements. The easiest method is to approximate $\langle T_{tr}(z) \rangle$ by air temperature (Thom, 1975), but this overestimates the storage flux, particularly in thick trunks in which a large fraction of the biomass is highly insulated. Otherwise, measurements within the woody biomass are performed. As discussed by Meesters and Vugts (1996), these can be used to evaluate J_{tr} if measurements are made through a whole tree section, as done by Aston (1985) and Lamaud et al. (2001). However, temperature measurements are more often made at one or two depths per species and radius class (see e.g. McCaughey and Saxton (1988), Moore and Fisch (1986) and Oliphant et al. (2004)), leading to estimates of J_{tr} which depend on the choice of these depths and, in the case of more than one depth, the averaging method.

In the absence of the full radial temperature profile, an estimate of J_{tr} requires consideration of the radial diffusion of heat within the trunks, as represented by the radial heat conduction equation for a cylinder:

$$\frac{\partial T_{tr}}{\partial t} = \kappa \left(\frac{\partial^2 T_{tr}}{\partial r^2} + \frac{1}{r} \frac{\partial T_{tr}}{\partial r} \right) \tag{6}$$

where κ is the thermal diffusivity of the trunk material and r is radial distance. Herrington (1969) employed a periodic solution of Eq. (6), to relate the heat flux density at the surface to the surface temperature, under the assumption of a sinusoidally varying surface temperature being equal to the surrounding air temperature. Moore and Fisch (1986) extended this method to include a surface resistance, thus avoiding Herrington's assumption of equal air and trunk surface temperatures. The solution was used to determine the depth within a trunk of given radius at which the measured temperature is in phase with the average vegetation temperature and could thus be used to generate a representative temperature for use in Eq. (5). Meesters and Vugts (1996) further extended the method of Herrington (1969) by use of an arbitrary (non-sinusoidal) temperature time-series using Fourier analysis, a more accurate correction for surface resistance and application to a forest with variable trunk diameter. Silberstein et al. (2003) applied the Force-Restore model (Deardorff, 1978; Lin, 1980) to tree trunks, using trunk temperature measurements at two depths to parameterize the model. Potter and Andresen (2002) and Jones et al. (2004) applied Eq. (6) to tree trunks by using finite difference schemes.

We seek a method for evaluating J_{tr} which is both widely applicable and readily implemented in a SVAT model with sub-diurnal time-resolution. Wide applicability requires that the model accounts for variable trunk diameter, is independent of trunk-temperature data and is computationally efficient. Of the above-mentioned approaches, only the Meesters and Vugts (1996) model satisfies all these criteria. It is also preferable that only variables (e.g. air temperature, modelled trunk temperature) from the previous SVAT model time step be stored during the computations. This is not the case for the approach of Meesters and Vugts (1996), which requires Fourier decomposition of a time series of temperature data.

In this work, we propose an alternative analytical solution to Eq. (6), which allows the radial trunk temperature profile at each time step to be calculated using only the trunk temperature profile from the previous time-step, the current air temperature and the current canopy radiation distribution. In Section 2, we describe this solution and its implementation in a multi-layer SVAT model. In Section 3 we apply the model to a 40 m tall Eucalyptus forest. Modelled and measured trunk temperatures are compared and the impact of canopy heat storage fluxes on hourly energy closure and modelled hourly above-canopy heat fluxes is assessed. In Section 4, modelled hourly biomass heat storage fluxes are compared with those predicted by the method of Meesters and Vugts (1996), and an adaptation of the Force-Restore method. Findings are summarized in Section 5.

2. A model for the estimation of the biomass heat storage flux

2.1. Analytical solution of the heat diffusion equation

We approximate the radial trunk temperature profile by that of an infinitely-long cylindrical section of trunk with some initial radial temperature profile that evolves over a given SVAT model time-step (centred at time t_k and of duration Δt), in response to heat diffusion within the trunk and exchange of heat and radiation between the trunk surface (at temperature $T_{tr,S}$) and the surrounding atmosphere (at temperature T_a). Heat diffusion is assumed to occur in the radial dimension only, as described by Eq. (6), with thermal diffusivity assumed independent of radius. Heat exchange between the trunk surface and the atmosphere occurs by convection, insolation and long-wave radiation, and is assumed to be uniform about the trunk circumference. Net shortwave and isothermal longwave radiation flux densities are summed to give the rate of net radiation absorption per unit area of trunk, $R^*_{net,tr}$, that would occur if the trunk temperature were equal to the ambient air temperature. The conductances to transport of sensible heat (h_c) and non-isothermal longwave radiation (h_r) are summed to give the surface conductance, h, which will be formulated in Section 2.2.2. It is assumed that, for the duration of each SVAT model time step, the external forcing variables (T_a, h, and $R^*_{net,tr}$) remain constant at their mean values for the time step. This assumption will be justified in Section 3.5.

It is convenient to rewrite Eq. (6) in terms of the difference between the trunk temperature (at time t and radius r) and air temperature:

$$\theta(t,r) = T_{tr}(t,r) - T_a$$

$$\frac{\partial\theta}{\partial t} = \kappa\left(\frac{\partial^2\theta}{\partial r^2} + \frac{1}{r}\frac{\partial\theta}{\partial r}\right) \tag{7}$$

The surface boundary condition is:

$$\left.\frac{\partial\theta}{\partial r}\right|_{r=R} = -\frac{h}{k}\theta(t,R) + \frac{R^*_{net,tr}}{k} \tag{8}$$

This is derived by equating the energy flux into the surface, $q(t)$, given by Fourier's law:

$$q(t) = kA\left.\frac{\partial\theta}{\partial r}\right|_{r=R} \tag{9}$$

and Newton's law of cooling (modified to account for the isothermal radiative heat flux, $R^*_{net,T}$):

$$q(t) = A(R^*_{net,tr} - h\theta(t,R)) \tag{10}$$

In Eqs. (8)–(10), R is the radius of the cylinder, A is the exposed surface area of the cylinder per unit area of ground, k is the thermal conductivity of the trunk material and $h = h_c + h_r$. The boundary condition at the centre of the cylinder ($r = 0$) is:

$$\left.\frac{\partial\theta}{\partial r}\right|_{r=0} = 0 \tag{11}$$

The solution to Eq. (7) is then:

$$\theta(t,r) = \sum_{n=1}^{\infty}(B_n e^{-\lambda_n^2\kappa t}J_0(\lambda_n r)) + \frac{R^*_{net,tr}}{h} \tag{12}$$

which is an extension of the solution for the radial temperature profile of a cylinder immersed in a fluid which undergoes a sudden change in temperature (see e.g. Chapman, 1984 p. 114–116). Here λ_n are solutions of the transcendental equation:

$$\lambda_n R\frac{J_1(\lambda_n R)}{J_0(\lambda_n R)} - \frac{hR}{k} = 0 \tag{13}$$

and J_0 and J_1 are the zero- and first-order Bessel functions of the first kind. We use the initial condition, $\theta(t_0, r) = f(r)$, to evaluate B_n:

$$f(r) - \frac{R^*_{net,tr}}{h} = \sum_{n=1}^{\infty}B_n J_0(\lambda_n r) \tag{14}$$

Following Chapman (1984), the orthogonality of $J_0(\lambda_n r)$ allows the coefficients, B_n, to be expressed as:

$$B_n = \frac{2/R^2 \int_0^R r(f(r) - R^*_{\mathrm{net,tr}}/h) J_0(\lambda_n r) dr}{J_0^2(\lambda_n R) + J_1^2(\lambda_n R)} \quad (15)$$

Substituting (15) into (12) gives the final solution:

$$\theta(t, r) = \frac{2}{R^2} \sum_{n=1}^{\infty} \left[e^{-\lambda_n^2 \kappa t} \frac{J_0(\lambda_n r)}{J_0^2(\lambda_n R) + J_1^2(\lambda_n R)} \times \int_0^R r\left(f(r) - \frac{R^*_{\mathrm{net,tr}}}{h}\right) J_0(\lambda_n r) dr \right] + \frac{R^*_{\mathrm{net,tr}}}{h} \quad (16)$$

Finally, the change in heat storage in the cylinder over the kth SVAT model time step, $J_{\mathrm{tr}}(t_k)$, is equated with the net surface energy flux, averaged over the time step:

$$J_{\mathrm{tr}}(t_k) = AR^*_{\mathrm{net,tr}} - \frac{A}{\Delta t} \int_{t_k - \Delta t/2}^{t_k + \Delta t/2} h_c \theta(t, R) dt - \frac{A}{\Delta t} \int_{t_k - \Delta t/2}^{t_k + \Delta t/2} h_r \theta(t, R) dt \quad (17)$$

In Eq. (17), the first term is the net isothermal radiation absorbed, the second term is the mean sensible heat flux into the surface, $-H_{\mathrm{tr}}(t_k)$ and the third term is the thermal component of the net longwave radiation absorption.

In the following sections, we will illustrate the use of Eqs. (16) and (17). In Section 2.2, trunk dimensions, thermal properties, surface conductance and net isothermal radiation absorption are estimated, while details for evaluating λ_n and $f(r)$ are given in Section 3.

2.2. Implementing calculation of J_c in a SVAT model

We incorporate the calculation of J_c in the multi-layered canopy model originally developed by Leuning et al. (1995), with improvements described by Wang and Leuning (1998). The core of the model is a leaf-level model that couples stomatal conductance, photosynthesis and energy partitioning in response to atmospheric water vapour pressure deficit and water availability from the soil. A radiation sub-model, based on the approximations of Goudriaan and van Laar (1994) is used to calculate the rates of radiation absorption by sunlit and shaded leaves and the soil in the visible, near-infrared and thermal wavebands. This radiation sub-model has been extended, as described in Section 2.2.1, to include trunk and leaf area as separate components of the total vegetation area, enabling estimation of $R^*_{\mathrm{net,tr}}$. For the purpose of this study, a two-layer soil model (Choudhury and Monteith, 1988) is used to calculate fluxes of heat into the soil and air and soil evaporation. Respiration rates as a function of soil and air temperature are obtained by parameterisations for soil and biomass (Keith, pers. comm.). Turbulent transport within the canopy is modelled using the localised near field theory of Raupach (1989).

The model canopy is divided into n layers, with the ith layer having depth Δz_i and specified increments in cumulative leaf area and cumulative trunk area: $\Delta\xi_{\mathrm{L},i}$ and $\Delta\xi_{\mathrm{tr},i}$. $J_{\mathrm{tr},i}$ and $H_{\mathrm{tr},i}$ are evaluated from Eq. (17), with the surface area, A, replaced by $\Delta\xi_{\mathrm{tr},i}$. Height-dependent variables required for the evaluation of $H_{\mathrm{tr},i}$ and $J_{\mathrm{tr},i}$ are the net isothermal radiation, $R^*_{\mathrm{net,tr}}$ and the surface conductances for convective and radiative heat transfer (h_c and h_r). The procedures used to estimate these variables and the trunk radius, $R(z)$, are given below.

2.2.1. Net isothermal radiation absorbed by trunks

The net isothermal radiation absorbed by the trunks, $R^*_{\mathrm{net,tr}}$, is the sum of the short-wave component, $S_{\mathrm{net,tr}}$, and the isothermal longwave component,$B^*_{\mathrm{net,tr}}$. Each of these is evaluated separately within the radiation sub-model in which the total vegetation area index is separated into leaf and trunk components ($\Lambda = \Lambda_{\mathrm{L}} + \Lambda_{\mathrm{tr}}$), as is the cumulative vegetation area index ($\xi = \xi_{\mathrm{L}} + \xi_{\mathrm{tr}}$).

Short wave radiation absorption by trunks at canopy-depth ξ is obtained by summing over two wavebands (visible and near infrared), each of which is a weighted mean of the values for sunlit and shaded trunk areas. The rate of solar radiation absorption per unit cumulative vegetation area is the sum of the leaf and trunk components, weighted by area. For example, the absorption of non-beam-scattered diffuse radiation is:

$$Q_d(\xi) = \frac{(Q_{\mathrm{d,L}}(\xi)\Delta\xi_{\mathrm{L}} + Q_{\mathrm{d,tr}}(\xi)\Delta\xi_{\mathrm{tr}})}{\Delta\xi} \quad (18)$$

Radiation absorption per unit trunk area is the negative derivative of the net downward diffuse radiation flux with respect to cumulative trunk area:

$$Q_{\mathrm{d,tr}}(\xi) = -\frac{d}{d\xi_{\mathrm{tr}}}(I_{d0}(1 - \alpha^{\mathrm{eff}}_{\mathrm{cd}})e^{-k'_d \xi}) \quad (19)$$

Here I_{d0} is the incident flux of diffuse radiation; $\alpha^{\mathrm{eff}}_{\mathrm{cd}}$ is the effective reflection coefficient for the canopy (including soil) for diffuse radiation and k'_{d} is the extinction coefficient for diffuse radiation by vegetation. If we make the over-simplifying assumption that throughout the canopy ξ_L/ξ_{tr} is constant, then k'_d is the mean of the corresponding trunk- and leaf-specific coefficients, weighted by cumulative area:

$$k'_d = \frac{(k'_{d,L}\xi_L + k'_{d,tr}\xi_{tr})}{\xi} \tag{20}$$

Combining Eqs. (19) and (20), the diffuse radiation absorbed per unit trunk area is given by:

$$Q_{d,tr}(\xi) = I_{d0}k'_{d,tr}(1-\alpha_{cd}^{eff})e^{-k'_d\xi} \tag{21}$$

Similarly for leaves:

$$Q_{d,L}(\xi) = I_{d0}k'_{d,L}(1-\alpha_{cd}^{eff})e^{-k'_d\xi} \tag{22}$$

Full details of the solar-radiation sub-model are given in Appendix A. An alternative formulation which allows for varying ξ_L/ξ_{tr} with canopy depth is desirable and could be obtained via numerical solution of the two-stream radiation scheme (Sellers, 1985), but that is beyond the scope of this work.

The net long-wave radiation absorbed per m^2 of trunk area is estimated as:

$$\begin{aligned} B_{net,tr}(\xi) &= k_{d,tr}\varepsilon_{tr}(\sigma\varepsilon_{air}T_a^4 - \sigma\varepsilon_{tr}T_{tr,S}^4)e^{-k_d\xi} \\ &\quad + k_{d,tr}\varepsilon_{tr}(\sigma\varepsilon_{soil}T_a^4 - \sigma\varepsilon_{tr}T_{tr,S}^4)e^{-k_d(\Lambda-\xi)} \end{aligned} \tag{23}$$

where ε_{tr} is the emissivity of the trunk, ε_{air} is the apparent emissivity for a hemisphere radiating at air temperature, T_{tr} and T_{soil} are the trunk and soil surface temperatures, σ is the Stefan–Boltzmann constant and k_d is the extinction coefficient for diffuse radiation by black (non-scattering) canopy elements. All temperatures are in K. The first term in Eq. (23) is the net radiation absorbed by trunks due to long-wave radiation exchange between the trunks and the atmosphere, while the second term is the net radiation absorbed by trunks due to long-wave radiation exchange between the trunks and the soil. By linearising $T_{tr,S}^4$,

$$T_{tr,S}^4 = (T_a + (T_{tr,S} - T_a))^4 \approx T_a^4 + 4T_a^3\Delta T \tag{24}$$

where $\Delta T = T_{tr,S} - T_a$, we can rewrite $B_{net,tr}$ as the sum of isothermal and trunk-temperature-dependent components:

$$\begin{aligned} B_{net,tr}(\xi) &= \varepsilon_{tr}\sigma T_a^4 k_{d,tr}(\varepsilon_{air} - \varepsilon_{tr})e^{-k_d\xi} \\ &\quad + \varepsilon_{tr}\sigma k_{d,tr}(\varepsilon_{soil}T_{soil}^4 - \varepsilon_{tr}T_a^4)e^{-k_d(\Lambda-\xi)} \\ &\quad - 4\sigma\varepsilon_{tr}T_a^3 k_{d,tr}(e^{-k_d\xi} + e^{-k_d(\Lambda-\xi)})\Delta T \\ &= B^*_{net,tr}(\xi) - h_r(\xi)\Delta T \end{aligned} \tag{25}$$

where:

$$\begin{aligned} B^*_{net,tr} &= \varepsilon_{tr}\sigma T_a^4 k_{d,tr}(\varepsilon_{air} - \varepsilon_{tr})e^{-k_d\xi} \\ &\quad + \varepsilon_{tr}\sigma k_{d,tr}(\varepsilon_{soil}T_{soil}^4 - \varepsilon_{tr}T_a^4)e^{-k_d(\Lambda-\xi)} \end{aligned} \tag{26}$$

is the rate of absorption of isothermal net long-wave radiation by trunks and;

$$h_r(\xi) = 4\sigma\varepsilon_{tr}T_a^3 k_{d,tr}(e^{-k_d\xi} + e^{-k_d(\Lambda-\xi)}) \tag{27}$$

is the radiation conductance. (Note that $B^*_{net,tr}$is the longwave component of $R^*_{net,tr}$and that $R^*_{net,tr}$ is thus independent of trunk temperature.)

2.2.2. Surface conductance of trunks

The surface conductance, h, is the sum of radiative and convective heat transfer coefficients, $h = h_r + h_c$, with h_r defined above in Eq. (27). The convective heat transfer coefficient is the sum of forced- and free-convection components. The coefficients for convection for a cylinder are given by Monteith and Unsworth (1990). For forced convection, $h_{c,forced} = \rho c_p D_h Nu_{forced}/2R$, while for free convection, $h_{c,free} = \rho c_p D_h Nu_{free}/L$. Here D_h is the molecular diffusivity for heat in air and L is the trunk height. The Nusselt number formulation is different for forced and free convection: $Nu_{forced} = 0.17\,Re^{0.62}$ $(4\times10^3 < Re < 4\times10^4)$ or $Nu_{forced} = 0.024\,Re^{0.81}$ $(4\times10^4 < Re < 4\times10^5)$ and $Nu_{free} = 0.11\,Gr^{0.33}$ $(10^4 < Gr < 10^9)$ or $Nu_{free} = 0.58\,Gr^{0.25}(10^9 < Gr < 10^{12})$. Here Gr is the Grashof number: $Gr = 1.58\times10^8\,L^3\Delta T$.

2.2.3. Trunk radius distribution

To estimate $J_{tr,i}$ at each canopy layer, we require an estimate of some mean trunk radius and its height dependence. (Note that here we include branches in our definition of trunk.) Meesters and Vugts (1996) concluded that the mass-weighted average radius provides enough information for this purpose. This is given by the quadratic mean radius:

$$\overline{R}(z) = \sqrt{\frac{\sum_j (R_j(z))^2}{n}} \tag{28}$$

where n is the number of radius classes and $R_j(z)$ is the trunk radius of the jth radius class at height z within the canopy. We estimate $R_j(z)$ from Frumau (1993), as quoted by Meesters and Vugts (1996):

$$\frac{z}{h_{tr,j}} = 0.44 + 0.50\cos\left(4.6\frac{R_j(z)}{d_{bh,}}\right) \tag{29}$$

where $h_{tr,j}$ and $d_{bh,j}$ are the tree height and diameter at breast height corresponding to the jth radius class. The vertical trunk area distribution is obtained by evaluating the exposed surface area of the cylinder in each vertical layer:

$$\Delta\xi_{T,i} = 2\pi\overline{R}(z_i)n_{tr}\Delta z_i \quad (30)$$

where n_{tr} is the number density of trees.

3. Model results

The SVAT model, forced by hourly local meteorological data, was used to calculate fluxes of sensible heat, latent heat and CO_2 above a temperate Eucalyptus forest at the Tumbarumba Ozflux site in southeast Australia (Leuning et al., 2005). Heat storage fluxes in the air column were obtained from measured water vapour and temperature profiles at seven heights within and above the canopy. Measurement details are given by Leuning et al. (2005). The model canopy was divided into 20 layers. The leaf area distribution (and hence $\Delta\xi_{L,i}$) was approximated by assuming that the leaf area of the understorey (1.0 m^2 (leaf) m^{-2} (ground)) was evenly distributed in the lower 2 m, while the remaining leaf area (2.5 m^2 (leaf) m^{-2} (ground)) was distributed according to measured vertical leaf area density distribution (D.L.B. Jupp, personal communication). Trunk area distribution was calculated via Eqs. (29) and (30), which require diameters at breast height and heights of trees. Diameters at breast height (d_{bh}) were measured for all 888 trees contained within 30 × 1 ha measurement plots (corresponding to a number density, n_{tr}, of 0.030 trees per m^2) at the Tumbarumba site. Regression analysis on a subset of 241 trees indicated that tree height (in m) could be estimated from d_{bh} (in cm) *via*: $h_{tr,j} = 2.043 d_{bh,j}^{0.7177}$. An estimate of m_{tr} = 66 kg m^{-2} was recovered from $\overline{R}(z)$, using n_{tr} = 0.03 m^{-2} and ρ_{tr} = 1000 kg m^{-3}. This agrees within the uncertainty limits of an independent estimate of biomass (73 ± 8 kg m^{-2}) obtained by applying allometric equations derived from harvested trees to inventory data of tree diameter (H. Keith, unpublished data). This satisfactory agreement lends support to the general use of Eq. (29) to predict $R(z)$, although this expression was developed for pine trees.

Values of thermal properties of the trunks were assigned as follows. Trunk density, ρ_{tr}, was from measured values of dry sapwood and bark densities and their respective relative masses and water content. Specific heat capacity was calculated as the mean of values for cellulose and water, weighted by the densities of the dry wood and water, giving c_{tr} = 2760 J kg^{-1} K^{-1}. Thermal conductivity was estimated to be k = 0.32 W m^{-1} K^{-1}, using the following relation reported by Simpson and TenWolde (1999): $k = \rho_{tr,d} \times 10^{-3}(0.1941 + 0.00406M) + 0.01864$. Here $\rho_{tr,d}$ is the density of dry wood and M is the ratio of moisture mass to dry wood mass (in %). The value of k adopted here agrees well with the value of k = 0.38 ± 0.07 W m^{-1} K^{-1} used by Moore and Fisch (1986) for trunks in a tropical Amazonian forest. Combined, the above thermal properties give a thermal diffusivity, $\kappa = k/\rho_{tr}c_{tr}$, of 1.14 × 10^{-7} m^2 s^{-1}. Based on reflectance spectra measured at Tumbarumba (D.L.B. Jupp, personal communication), α_{tr} was taken as 0.2 and 0.4 for the visible and NIR wavebands respectively. Trunk emissivity, ε_{tr}, was set to 0.94. The sensitivity of J_{tr} to κ, ρ_T and ε_{tr} is evaluated in Section 3.4.

The SVAT model was run at an hourly time-step, with hourly average forcing data. At each SVAT time step (centred at t_k and duration Δt = 1 h), the trunk temperature distribution was evaluated by Eq. (16) at 10 evenly-spaced radii from the trunk core to the surface, and at 5 evenly-spaced time points from $t = t_k - \Delta t/2$ to $t = t_k + \Delta t/2$. Values of λ_n for use in Eq. (16) were obtained by using a root-finding method to solve Eq. (13). Five terms in the summation in Eq. (16) were sufficient for convergence. The initial condition $f(r)$ was defined by the trunk temperature distribution at the end of the previous time step, $f(r) = T_{tr,S}(t_{k-1} + \Delta t/2, r) - T_a$.

3.1. Magnitude of the canopy heat storage flux

Fig. 1 illustrates the hourly-resolved components of the canopy heat storage flux for a typical clear-sky 24 h period in March 2005 at Tumbarumba. The canopy heat

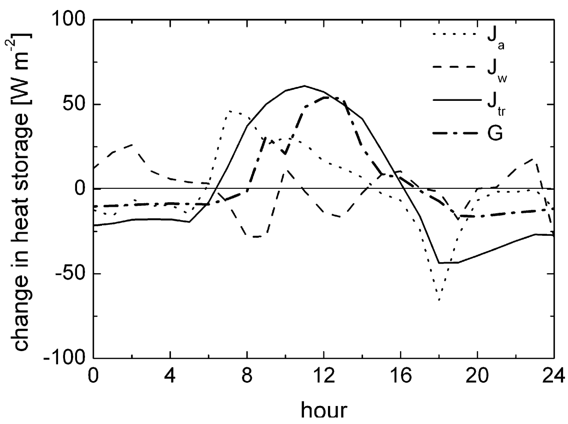

Fig. 1. Hourly components of the canopy heat storage flux (J_a, J_w and J_{tr}), and the heat flux into the soil (G), for day 73, 2005 at Tumbarumba.

storage flux, J_c comprises contributions from J_{tr}, J_a and J_w which are of comparable magnitude but have very different time courses. J_a has maximum and minimum values (47 and -50 W m^{-2} respectively) in the early morning and late afternoon, corresponding to times when the canopy air temperature is changing most rapidly. In contrast J_{tr} has a later maximum of 61 W m^{-2} at about 11:00 h, owing to the significant contribution of solar radiation absorption. This peak value shows no significant seasonal variation over the model period (day 19–140), with a mean clear-sky maximum hourly value of $J_{tr,max} = 56 \pm 8$ W m^{-2}. The large contribution of $R^*_{net,T}$ to J_{tr} was further illustrated by an additional model run, in which radiative energy transfer to the trunks was completely switched off. This had the effect of lowering the maximum hourly values of J_{tr} from 61 to 23 W m^{-2}. The absolute magnitudes of J_P and J_l (not shown here) do not exceed 3 W m^{-2} and 2 W m^{-2} respectively, and are not considered further in this work. The canopy heat storage flux ($J_{tr} + J_a + J_w$) is large compared to the heat flux into the soil, G, which peaks at 48 W m^{-2} at 13:00 h. Here, G was obtained from measured values of the soil heat flux at $z = 0.05$ m depth, G_z, combined with the soil temperature, T_{soil} (mean of measured values at depths of 0.02 m and 0.05 m) and the volumetric soil heat capacity, C_s: $G = G_z + zC_S\Delta T_{soil}/\Delta t$.

The effects of both varying leaf area index and trunk diameter on maximum hourly values of J_{tr} are illustrated in Fig. 2. This contour diagram was produced from model predictions assuming a fixed biomass (wet wood) of 66 kg m^{-2} and with meteorological forcing data for day 73, 2005 at Tumbarumba (maximum solar radiation 978 W m^{-2} and air temperature range of 10 °C). The model was run for a range of leaf area indices (0–6) and $\overline{R}_{bh}$ (5–40 cm). (Note that a leaf area index of 3.5 and $\overline{R}_{bh}$ of 13 cm apply at the Tumbarumba site.) J_{tr} decreases significantly with $\overline{R}_{bh}$, since thicker trunks contain a higher proportion of insulated wood, and therefore undergo smaller changes in heat storage per unit of biomass. The decrease in J_{tr} with increasing leaf area index occurs because of the consequent decrease in $R^*_{net,tr}$. For a given $\overline{R}_{bh}$ and leaf are index, J_{tr} is proportional to biomass. Thus Fig. 2 provides a useful indication of the maximum hourly value of J_{tr} for a forest with known leaf area index, $\overline{R}_{bh}$ and biomass, on a cloudless day with a temperature range of 10 °C.

3.2. Comparison of model output with measured trunk temperatures

Fig. 3 shows that hourly trunk temperatures predicted by the model compare well with a time series of trunk temperature measurements obtained from thermocouples inserted at breast height 2 cm within the sapwood of a *Eucalyptus delegantensis* tree with $d_{bh} = 28.2$ cm. Here, model output was generated with $\overline{R}_{bh}$ set to that of the measured tree. The results at the depth of interest (taking account of bark thickness), along with the external air temperature measurements indicate that the model captures well the phase shift and damping of the temperature wave within the trunk. Linear regression analysis of modelled versus measured trunk temperatures over a longer period (day of year

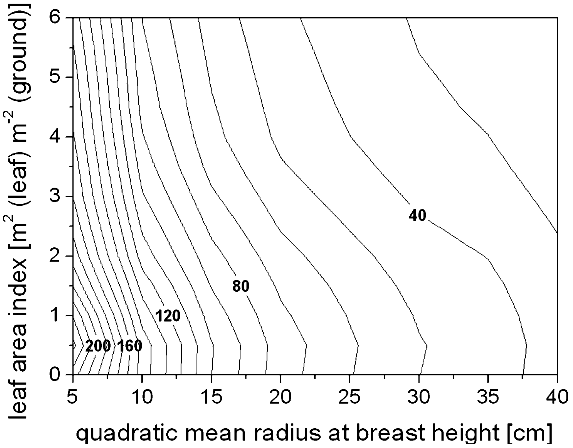

Fig. 2. Maximum hourly values of J_{tr}, calculated for range of leaf area indices and trunk radii, with meteorological forcing data for day 73, 2005 at Tumbarumba (clear sky with temperature range of 10 °C) and woody biomass 66 kg m^{-2} (dry).

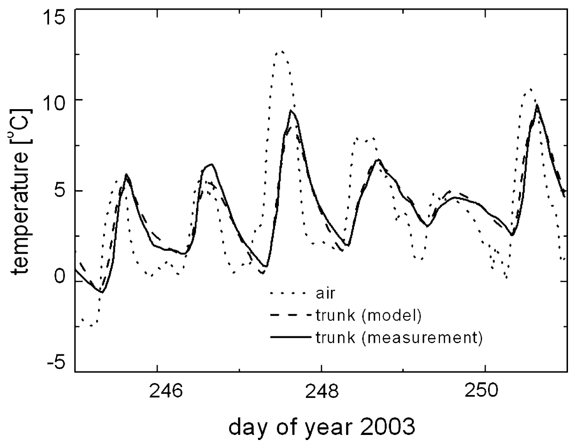

Fig. 3. Comparison of measured and modelled trunk temperatures over a 6-day period. Measurements were made at a height of 1.3 m, 2 cm within the sap-wood of a *Eucalyptus delegatensis* tree ($d_{bh} = 28.2$ cm). Air temperature is also shown, to illustrate the phase-shift and damping of the trunk-temperature wave.

238–276, 2003), gave: *n = 1745*; *slope = 0.87*; *intercept = 0.57 °C*; R^2 *= 0.94*; $P < 10^{-4}$. Contributions to residuals include: different thermal properties of the bark compared to wood; assumption of uniform $R^*_{\mathrm{net,tr}}$ around the trunk circumference; uncertainties in the thermal and radiation scattering properties of the wood and uncertainty in the position of thermocouples.

3.3. Applicability of biomass storage flux calculation to a single layer canopy model

We simulated the evaluation of J_{tr} within a single-layer model. For this purpose, forcing variables (i.e. T_{a}, $R^*_{\mathrm{net,tr}}$, h_{c}, h_{r}) were taken as the vertically averaged values from the multilayer model, weighted by incremental trunk area, $\Delta\xi_{\mathrm{tr,i}}$. The single-layer radius was taken as the quadratic mean value of the vertical radius profile. The resulting hourly values of J_{tr} differed from those of the multilayer model output by less than 5 W m^{-2}, indicating that the multilayer version of the biomass storage model can be condensed to a single layer without significant loss of accuracy. The good agreement lends further support to the assertion of Meesters and Vugts (1996) that a mass-weighted mean value of trunk radius is sufficient for the purpose of evaluating J_{tr}.

3.4. Sensitivity of modelled biomass storage flux to variations in parameters and time-step size

The contributions of uncertainties in the mean trunk radius at breast height, trunk albedo, thermal diffusivity and thermal emissivity ($\overline{R}_{\mathrm{bh}}$, α_{tr}, κ and $\varepsilon_{\mathrm{tr}}$) to the variance in J_{tr} were investigated by sensitivity analysis. The variance in J_{tr} attributable to the uncertainty in each parameter was calculated using the following uncertainty estimates: $\Delta_{\overline{R}_{\mathrm{bh}}} = 0.02\,\mathrm{m}$; $\Delta_{\alpha_{\mathrm{tr}}} = 0.1$; $\Delta\kappa = 2.5 \times 10^{-7}\,\mathrm{m}^2\,\mathrm{s}^{-1}$; $\Delta_{\varepsilon_{\mathrm{tr}}} = 0.05$. Fig. 4a shows that uncertainties in albedo radius and thermal diffusivity make comparable contributions to the error, while errors in emissivity are less consequential. Fig. 4b illustrates the combined uncertainty (grey shaded area), imposed on the calculation of J_{tr} for a typical clear-sky day in March 2005. The combined uncertainties in the parameters investigated here produce error bars (one standard deviation) on J_{tr} of < 15 W m^{-2}.

The analytical solution formulated in Section 2 assumes that the external forcing variables (air temperature, T_{a}, surface conductance, h, and net isothermal radiation, $R^*_{\mathrm{net,tr}}$) are constant for the duration of the SVAT model time-step. The consequences of this assumption were tested in a calculation using trunk area-weighted forcing variables stored from the SVAT model. The analytical solution evaluated with time-step 1 h was compared with the solution with time-step 5 min, using external forcing variables splined to this time-resolution. The results agreed to within 2 W m^{-2}, indicating that the assumption of step changes in h, $R^*_{\mathrm{net,T}}$ and T_{a} is not a serious source of error.

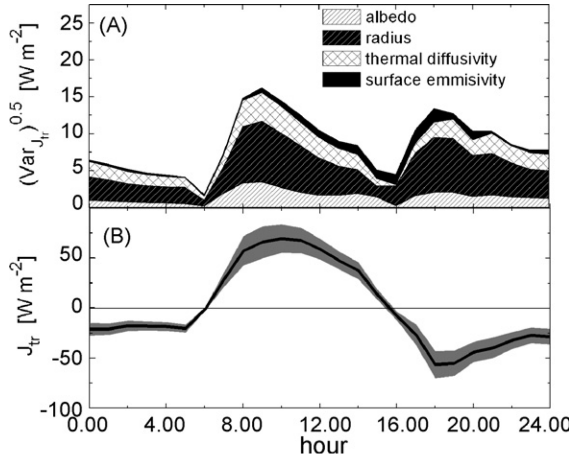

Fig. 4. (A) Components of variance attributable to uncertainty in trunk albedo, mass-weighted mean radius, thermal diffusivity and trunk surface emissivity. (B) Biomass storage flux (solid line), with 1σ uncertainty limits (shaded area) calculated as the sum of the components above. (Model output for day 73, 2005 at Tumbarumba).

3.5. Effects of including canopy storage flux on energy closure and modelled above-canopy heat fluxes

We now present model output that demonstrates the effect of including J_{c} in the hourly energy budget. The SVAT model was run for the period spanning days 19-140 of 2005 for Case A that excluded all components of J_{c}, and for Case B that included heat storage fluxes into the air column and biomass (J_{a}, J_{w} and J_{tr}). The results are summarized in Table 1. The parameters m and b are the slopes and intercepts of the geometric mean regression lines (Sokal and Rohlf, 1995), fitted to sets of 2928 pairs of modelled and measured hourly fluxes of latent heat, sensible heat, carbon dioxide and net radiation (λE, H, $F_{\mathrm{CO_2}}$ and R_{net}). Energy closure is denoted by Ω, and here, m is the slope of the linear regression (forced through zero) between the sum of measured sensible and latent heat fluxes and the available energy. Available energy is defined as: $(R_{\mathrm{net}} - G)$ for Case A and $(R_{\mathrm{net}} - G - J_{\mathrm{a}} - J_{\mathrm{w}} - J_{\mathrm{tr}})$ for Case B. All correlations were significant at $P < 10^{-4}$.

Table 1
Geometric mean regression slopes and intercepts relating modelled and measured fluxes (H, λE, F_{CO_2}, R_{net}), and linear regression slope for energy closure (Ω)

Case	Quantity	m	b	R^2
A ($J_c = 0$)	H (W m^{-2})	1.08 ± 0.01	-35 ± 1.0	0.79
	λE (W m^{-2})	0.97 ± 0.01	5 ± 1.0	0.74
	F_{CO_2} (mg m^{-2} s^{-1})	1.09 ± 0.01	-0.043 ± 0.003	0.86
	R_{net} (W m^{-2})	0.894 ± 0.002	-3.2 ± 0.2	0.99
	Ω	0.904 ± 0.005	0	0.88
B ($J_c = J_w + J_a + J_{tr}$)	H (W m^{-2})	0.98 ± 0.01	-16.5 ± 0.8	0.81
	λE (W m^{-2})	1.00 ± 0.01	-1.5 ± 1.1	0.73
	F_{CO_2} (mg m^{-2} s^{-1})	1.02 ± 0.01	-0.050 ± 0.003	0.84
	R_{net} (W m^{-2})	1.010 ± 0.001	-0.9 ± 0.2	0.99
	Ω	1.01 ± 0.01	0	0.87

Scatter plots for energy closure and sensible heat flux are shown in Fig. 5. Accounting for J_c in the available energy budget significantly improves hourly energy closure, with the slope of the linear regression of measured heat flux against available energy increasing from 0.90 to 1.01. Thus, at the Tumbarumba site, inclusion of J_c addresses the "energy closure problem", whereby Ω is commonly found to be significantly less than 1 (e.g. Blanken et al., 1997; Oliphant et al., 2004; Wilson et al., 2002). Incorporation of J_c also improves agreement for H, decreasing the slope from 1.08 to 0.98 and reducing the bias from -35 to -16.5 W m^{-2}. Inclusion of trunks in the radiation sub-model has the significant effect of increasing modelled R_{net}, with the slope increasing from 0.89 to 1.01. This is because the trunk area here (0.9 m^2 (trunk) m^{-2} (ground)) is significant compared to the leaf area index and trunks have lower scattering coefficients than leaves.

4. Comparison with alternative methods for estimating J_{tr}

We compared the analytical solution described in Section 2, with two other methods: the method of Meesters and Vugts (1996), and a variant of the Force-Restore method, commonly used to estimate the net heat flux into the soil (Deardorff, 1978; Lin, 1980). The method of Meesters and Vugts is a solution to the heat conduction Eq. (6), with a surface boundary condition imposed by assuming periodic variation in air temperature, T_a. Periods of arbitrary length are allowed for by performing a Fourier decomposition on the T_a time series. A limitation of this method is that it does not incorporate radiative heat transfer by either long-wave energy exchange or by insolation. The Force-Restore method employs a periodic solution of the equation for one-dimensional heat diffusion in an infinite slab to describe the time evolution of the deep soil temperature and the mean temperature in a thin surface layer. Silberstein et al. (2003) adapted the Force-Restore equations (Lin, 1980) for trunks, replacing G by J_{tr} and the two soil layers with an outer and inner layer of the trunk, referred to as "bark" and "core":

$$\frac{\partial T_{bark}}{\partial t}\left(1+\frac{\delta_{tr}}{d}\right) = \frac{2\sqrt{\pi}J_{tr}}{A_{tr}\rho_{bark}c_{bark}\sqrt{\kappa_{bark}\tau_{bark}}} - \frac{2\pi}{\tau_{bark}}(T_{bark}-T_{core}) \tag{31}$$

$$\frac{\partial T_{core}}{\partial t} = \frac{\sqrt{\pi}J_{tr}}{A_{tr}\rho_{core}c_{core}\sqrt{\kappa_{core}\tau_{core}}} \tag{32}$$

where δ_{tr} is the thickness of the outer layer, d is the damping depth of the diurnal temperature wave, A is the trunk surface area and τ_{bark} and τ_{core} are the time constants for the outer and inner layers. Silberstein et al. (2003) used temperature measurements at two depths to obtain parameters in Eqs. (31) and (32). In contrast, we propose an alternative implementation of the method, requiring as input the same parameters and forcing data as required for the analytical solution of Eq. (6), and no temperature measurements. We use the limiting case $\delta_{tr} \to 0$ (as done by Deardorff (1978) for soils), so that T_{bark} becomes the trunk surface temperature, $T_{tr,S}$. This is convenient because it eliminates the need to define a skin thickness and because J_{tr} can be expressed in terms of $T_{tr,S}$:

$$J_{tr}(t) = A(R^*_{net,tr}(t) + h(t)(T_a(t) - T_{tr,S}(t))) \tag{33}$$

In the Force-Restore method for soils, the time-constants for the surface and deep soil layers are the diurnal period (24 h) and the annual period (365 d). Since the damping depth of the annual temperature

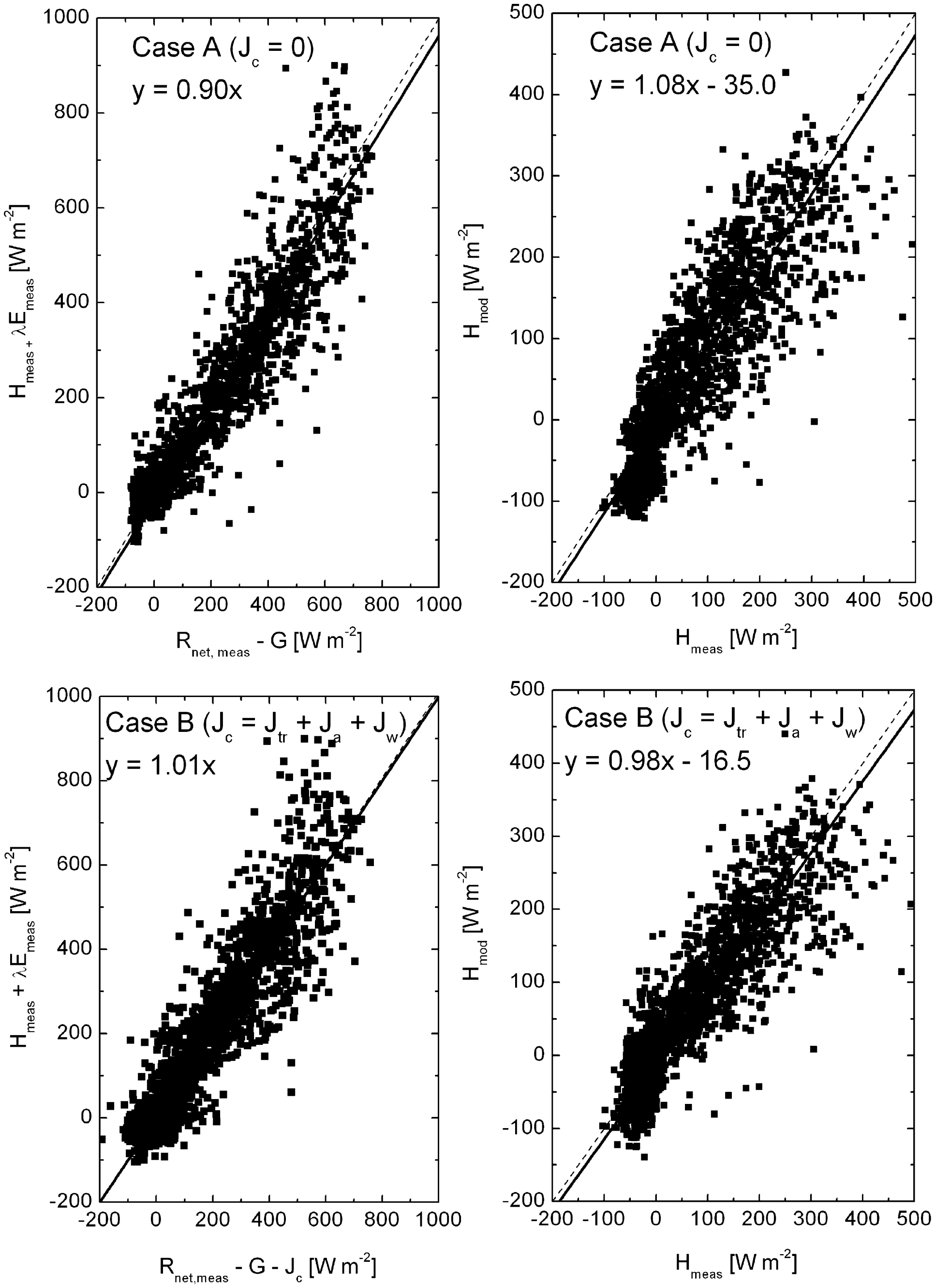

Fig. 5. Scatter plots of energy closure (left) and modelled against measured sensible heat fluxes (right) for the Tumbarumba site (day 19–140, 2005). Case A (top) excludes and Case B (bottom) includes the canopy heat storage flux. Dashed lines are the 1:1 lines and solid lines are the linear fits.

wave in trunks is >1 m (significantly deeper than the core of the trunk) the effect of the annual temperature wave on J_{tr} can be ignored. We therefore set τ_{core} to the diurnal period, τ, thereby specifying T_{core} as the depth-averaged temperature between the surface and the diurnal damping depth (~6 cm). Incorporating the above modifications, Eqs. (31) and (32) become:

$$\frac{\partial T_{tr}}{\partial t} = \frac{2\sqrt{\pi}(R^*_{net,tr}(t) + h(t)(T_a(t) - T_{tr,S}(t)))}{\rho_{tr} c_{tr} \sqrt{\kappa\tau}} - \frac{2\pi}{\tau}(T_{tr,S} - T_{core}) \quad (34)$$

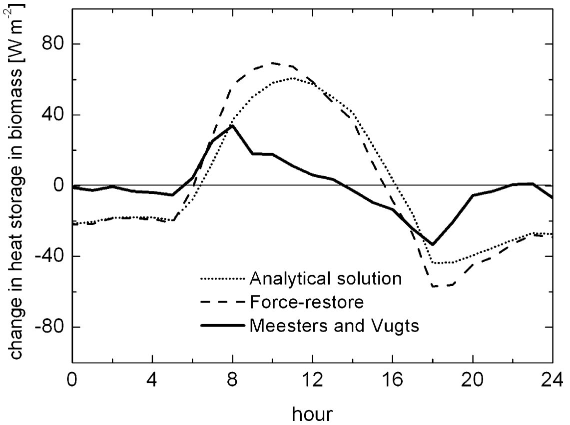

Fig. 6. Modelled biomass heat storage flux for day 73, 2005 at Tumbarumba, using the analytical solution (this work), the method of Meesters and Vugts (1996), and the Force-Restore method, adapted for trunks.

$$\frac{\partial T_{\text{core}}}{\partial t} = \frac{\sqrt{\pi}(R^*_{\text{net,tr}}(t) + h(t)(T_{\text{a}}(t) - T_{\text{tr,S}}(t)))}{\rho_{\text{tr}} c_{\text{tr}} \sqrt{\kappa \tau}} \qquad (35)$$

which are readily rewritten in finite-difference form.

An approximation of the Force-Restore method applied to trunks is that it is formulated in rectangular rather than cylindrical co-ordinates. The effect of this approximation was investigated by evaluating the numerical solution of Eq. (6) using both rectangular and cylindrical co-ordinates. The results agree within 7 W m^{-2}, indicating that the approximation is reasonable in this instance.

Results of the Force-Restore method, the Meesters and Vugts method and the analytical solution developed here are compared in Fig. 6. It is clear that, compared with the analytical solution, the Meesters and Vugts method significantly underestimates the amplitude of the biomass heat storage flux with the peak value of 33 W m^{-2} occurring earlier in the morning at about 08:00 h. This is because this model neglects heat transfer by radiation. The maximum discrepancy is 50 W m^{-2}, occurring at about 12:00 h. In contrast, the Force-Restore method agrees remarkably well with the analytical solution developed here. The peak value of 68 W m^{-2} is slightly higher and occurs slightly earlier (at 10:00 h) than that of analytical solution. The maximum discrepancy is 18 W m^{-2} and occurs at 08:00 h.

5. Summary and conclusions

An analytical solution to the heat conduction equation has been demonstrated as an effective method for calculation of J_{tr} within the framework of a SVAT model. Model output for the tall forest at the Tumbarumba site shows that accounting for J_{c} in the energy budget improves agreement between hourly available energy and the sum of latent and sensible heat fluxes measured above the canopy. At Tumbarumba, J_{tr} is a large component of J_{c}, with maximum hourly values on cloudless days of 56 ± 8 W m^{-2} which show no seasonality and occur at about 11:00 h. For a given biomass, peak values of J_{tr} increase steeply with decreasing trunk radius and decreasing leaf area index (due to increasing radiation absorbed by the trunk). These effects have been quantified and are summarized in Fig. 2, enabling a rapid estimate of peak hourly clear-sky values of J_{tr} for a forest of given woody biomass, quadratic mean trunk radius and leaf area index. Sensitivity analysis shows that variance in hourly J_{tr} due to uncertainties in trunk albedo, emissivity and thermal diffusivity and mean radius is less than 15 W m^{-2}, and agreement to within 1 °C between modelled and measured trunk temperatures provides model validation. Significant advantages of this model over previous approaches are: (1) it is independent of biomass temperature measurements; (2) only variables from the previous SVAT model time step need to be stored; (3) effects of radiative heat transfer, shown here to be significant, are readily included via the surface boundary condition. The Force-Restore method also has these advantages. Despite the additional approximations of this method (rectangular co-ordinates, only two layers and periodic temperature variation) it predicts hourly values of J_{tr} which agree well (to within 18 W m^{-2} on a cloudless day at Tumbarumba) with the analytical solution of the more detailed model presented here. The simplicity and computational efficiency of the Force-Restore method make it an attractive alternative in situations where this level of agreement is acceptable.

Appendix A

A.1. Radiation sub-model: rates of radiation absorption

We adapt the method of Goudriaan and van Laar (1994) to evaluate rates of solar radiation absorption by leaves and trunks. Short wave radiation absorption by trunks at canopy-depth ξ is obtained by summing over two wavebands (visible and near infrared), each of which is a weighted mean of the values for sunlit and shaded trunk areas:

$$S_{\mathrm{net,tr}}(\xi) = \sum_{j=1}^{2} (f_{\mathrm{sl}}(\xi) Q^j_{\mathrm{sl,tr}}(\xi) + f_{\mathrm{sh}}(\xi) Q^j_{\mathrm{sh,tr}}(\xi)) \quad (36)$$

where f_{sl} and f_{sh} are the fractions of sunlit and shaded vegetation area and j denotes the waveband. The absorptions of visible and infrared radiation are calculated separately because separate scattering coefficients apply. However, the calculations are otherwise identical and the superscript j is omitted in the following equations.

The rate of solar radiation absorbed per m^2 of shaded vegetation is the sum of absorptions of diffuse radiation generated by incident diffuse and beam radiation: $Q_{\mathrm{sh}}(\xi) = Q_{\mathrm{d}}(\xi) + Q_{\mathrm{b,d}}(\xi)$. Q_{d} is the absorption of the incident diffuse radiation flux, which is complementary to transmission:

$$Q_{\mathrm{d}}(\xi) = -\frac{dI_{\mathrm{d}}(\xi)}{d\xi} = I_{\mathrm{d0}} k'_{\mathrm{d}} (1 - \rho^{\mathrm{eff}}_{\mathrm{cd}} e^{-k'_{\mathrm{d}}\xi}) \quad (37)$$

and $Q_{\mathrm{b,d}}$ is the absorption of scattered beam radiation (i.e. absorption of the flux generated by incident beam radiation, minus the absorbed fraction $(1 - \omega)$ of the direct beam):

$$Q_{\mathrm{b,d}}(\xi) = I_{\mathrm{b0}} k'_{\mathrm{b}} (1 - \alpha^{\mathrm{eff}}_{\mathrm{cb}}) e^{-k'_{\mathrm{b}}\xi} - I_{\mathrm{b0}} k_{\mathrm{b}} (1 - \omega) e^{-k_{\mathrm{b}}\xi} \quad (38)$$

Sunlit canopy elements absorb the same amount of diffuse radiation as shaded elements, as well as the absorbed fraction of the intercepted direct beam:

$$Q_{\mathrm{sl}}(\xi) = Q_{\mathrm{b}} + Q_{\mathrm{sh}}(\xi) = k_{\mathrm{b}} I_{\mathrm{b0}} (1 - \omega) + Q_{\mathrm{sh}}(\xi) \quad (39)$$

In Eqs. (37)–(39), I_{d0} and I_{b0} are the incident fluxes of diffuse and beam radiation; I_{d} is the net downward flux of diffuse radiation; k'_{d} and k'_{b} are the canopy extinction coefficients for diffuse and beam radiation; k_{d} and k_{b} are the canopy extinction coefficients for diffuse and beam radiation for hypothetical black (i.e. non-scattering) canopy elements; ω is the vegetation scattering coefficient; $\alpha^{\mathrm{eff}}{}_{\mathrm{cd}}$ and $\alpha^{\mathrm{eff}}{}_{\mathrm{cb}}$ are the effective canopy + soil reflection coefficients for incident diffuse and beam radiation.

The leaf- and trunk-specific rates of solar radiation absorption are:

$$Q_{\mathrm{d,L}}(\xi) = I_{\mathrm{d0}} k'_{\mathrm{d,L}} (1 - \alpha^{\mathrm{eff}}_{\mathrm{cd}}) e^{-k'_{\mathrm{d}}\xi} \quad (40)$$

$$Q_{\mathrm{d,T}}(\xi) = I_{\mathrm{d0}} k'_{\mathrm{d,tr}} (1 - \alpha^{\mathrm{eff}}_{\mathrm{cd}}) e^{-k'_{\mathrm{d}}\xi} \quad (41)$$

$$Q_{\mathrm{b,d,L}}(\xi) = I_{\mathrm{b0}} k'_{\mathrm{b,L}} (1 - \alpha^{\mathrm{eff}}_{\mathrm{cb}}) e^{-k'_{\mathrm{b}}\xi} - I_{\mathrm{b0}} k_{\mathrm{b,L}} (1 - \omega_{\mathrm{L}}) e^{-k_{\mathrm{b}}\xi} \quad (42)$$

$$Q_{\mathrm{b,d,T}}(\xi) = I_{\mathrm{b0}} k'_{\mathrm{b,tr}} (1 - \alpha^{\mathrm{eff}}_{\mathrm{cb}}) e^{-k'_{\mathrm{b}}\xi} - I_{\mathrm{b0}} k_{\mathrm{b,tr}} (1 - \rho_{\mathrm{tr}}) e^{-k_{\mathrm{b}}\xi} \quad (43)$$

$$Q_{\mathrm{b,L}} = k_{\mathrm{b,L}} I_{\mathrm{b0}} (1 - \sigma_{\mathrm{L}}) \quad (44)$$

$$Q_{\mathrm{b,tr}} = k_{\mathrm{b,tr}} I_{\mathrm{b0}} (1 - \alpha_{\mathrm{tr}}) \quad (45)$$

$$Q_{\mathrm{sh,L}}(\xi) = Q_{\mathrm{d,L}}(\xi) + Q_{\mathrm{b,d,L}}(\xi) \quad (46)$$

$$Q_{\mathrm{sh,tr}}(\xi) = Q_{\mathrm{d,tr}}(\xi) + Q_{\mathrm{b,d,tr}}(\xi) \quad (47)$$

$$Q_{\mathrm{sl}}(\xi) = Q_{\mathrm{b,L}} + Q_{\mathrm{sh,L}}(\xi) \quad (48)$$

$$Q_{\mathrm{sl,tr}}(\xi) = Q_{\mathrm{b,tr}} + Q_{\mathrm{sh,tr}}(\xi) \quad (49)$$

where the subscripts L and tr denote specificity to leaves and trunks respectively and ρ_{tr} is the trunk reflectance.

The relations between the leaf- and trunk-specific extinction and reflection coefficients and the canopy extinction and reflection coefficients must be defined such that each of Q_{d}, $Q_{\mathrm{b,d}}$ and Q_{b} (and hence Q_{sl} and Q_{sh}) are the mean values of the separate leaf and trunk components, weighted by area. If we make the over-simplifying assumption that throughout the canopy $\xi_{\mathrm{L}}/\xi_{\mathrm{tr}}$ is constant, then the condition above is satisfied if each canopy extinction coefficient (k_{b}, k_{b}' and k_{d}) is the mean of the corresponding trunk- and leaf-specific coefficients, weighted by area, and the canopy scattering coefficient is given by:

$$\omega = 1 - \frac{(1 - \omega_{\mathrm{L}}) k_{\mathrm{b,L}} \Lambda_{\mathrm{L}} + (1 - \alpha_{\mathrm{tr}}) k_{\mathrm{b,tr}} \Lambda_{\mathrm{tr}}}{k_{\mathrm{b,L}} \Lambda_{\mathrm{L}} + k_{\mathrm{b,tr}} \Lambda_{\mathrm{tr}}} \quad (50)$$

A.2. Radiation sub-model: extinction coefficients

Beam extinction coefficients for hypothetical black leaves and trunks are equivalent to the projected area on the ground of a unit area of vegetation, given by:

$$k_{\mathrm{b,L}} = G_{\mathrm{L}}/\cos\theta \quad (51)$$

$$k_{\mathrm{b,tr}} = G_{\mathrm{tr}}/\cos\theta \quad (52)$$

where G_{L} and G_{tr} are the unit area projections of leaves and trunks respectively in the direction of the beam and θ is the solar zenith angle. For trunks, we assume a vertical angle distribution (Ross, 1981):

$$G_{\mathrm{tr}} = \sin\theta/\pi, \quad (53)$$

while for leaves, we use the Ross-Goudriaan function (Sellers, 1985).

Beam extinction coefficients for scattering elements are related to those for non-scattering elements by:

$$k'_{\mathrm{b,L}} = k_{\mathrm{b,L}}\sqrt{1-\omega_{\mathrm{L}}} \tag{54}$$

$$k'_{\mathrm{b,tr}} = k_{\mathrm{b,tr}}\sqrt{1-\alpha_{\mathrm{tr}}} \tag{55}$$

Beam extinction coefficients for total vegetation take the mean values of the trunk and leaf coefficients, weighted by area, e.g.:

$$k_{\mathrm{b}} = \frac{k_{\mathrm{b,tr}}\Lambda_{\mathrm{tr}} + k_{\mathrm{b,L}}\Lambda_{\mathrm{L}}}{\Lambda_{\mathrm{tr}}+\Lambda_{\mathrm{L}}} \tag{56}$$

Absorption of incident diffuse radiation is approximated as the sum of the absorbed components from each of three zones centred at solar zenith angles of 15°, 45° and 75°, with weightings $w_{15} = 0.308$, $w_{45} = 0.514$ and $w_{75} = 0.178$ specified for the Standard Overcast Sky. The extinction coefficients for diffuse radiation in each zenithal zone are analogous to k_{b} and k_{b}'. For example:

$$k^{15}_{\mathrm{d,L}} = G_{\mathrm{L}}/\cos(15^{o}) \tag{57}$$

$$k^{15}_{\mathrm{d,tr}} = G_{\mathrm{tr}}/\cos(15^{o}) \tag{58}$$

$$k^{15}_{\mathrm{d}} = \frac{k^{15}_{\mathrm{d,tr}}\Lambda_{\mathrm{tr}} + k^{15}_{\mathrm{d,L}}\Lambda_{\mathrm{L}}}{\Lambda_{\mathrm{tr}}+\Lambda_{\mathrm{L}}} \tag{59}$$

$$k'_{\mathrm{d,L}}15 = k^{15}_{\mathrm{d,L}}\sqrt{1-\omega_{\mathrm{L}}} \tag{60}$$

$$k'_{\mathrm{d,tr}}15 = k^{15}_{\mathrm{d,L}}\sqrt{1-\rho_{\mathrm{tr}}} \tag{61}$$

$$k'_{\mathrm{d}}15 = \frac{k'_{\mathrm{d,tr}}15\Lambda_{\mathrm{tr}} + k'_{\mathrm{d,L}}15\Lambda_{\mathrm{L}}}{\Lambda_{\mathrm{tr}}+\Lambda_{\mathrm{L}}} \tag{62}$$

Effective extinction coefficients which apply across all three zenithal zones are defined by equating the two following expressions ((63) and (64)) for the attenuation of diffuse radiation by vegetation (leaves and trunks):

$$\frac{I_{\mathrm{d}}(\Lambda)}{I_{\mathrm{d},0}} = \frac{I^{15}_{\mathrm{d}}(\Lambda)}{I_{\mathrm{d},0}} + \frac{I^{45}_{\mathrm{d}}(\Lambda)}{I_{\mathrm{d},0}} + \frac{I^{75}_{\mathrm{d}}(\Lambda)}{I_{\mathrm{d},0}} = w_{15}e^{-k'_{\mathrm{d}}15\Lambda} + w_{45}e^{-k'_{\mathrm{d}}45\Lambda} + w_{75}e^{-k'_{\mathrm{d}}75\Lambda} \tag{63}$$

and,

$$\frac{I_{\mathrm{d}}(\Lambda)}{I_{\mathrm{d},0}} = e^{-k'_{\mathrm{d}}\Lambda} \tag{64}$$

This gives:

$$k'_{\mathrm{d}} = -\frac{1}{\Lambda}\ln\left(w_{15}e^{-k'_{\mathrm{d}}15} + w_{45}e^{-k'_{\mathrm{d}}45} + w_{75}e^{-k'_{\mathrm{d}}75}\right) \tag{65}$$

The rate of absorption of incident diffuse radiation by leaves at the bottom of the canopy can be expressed as the sum of components from the three zones:

$$Q_{\mathrm{d,L}}(\Lambda) = Q^{15}_{\mathrm{d,L}}(\Lambda) + Q^{45}_{\mathrm{d,L}}(\Lambda) + Q^{75}_{\mathrm{d,L}}(\Lambda) = (1-\alpha_{\mathrm{cd}})I_{\mathrm{d},0}\left(w_{15}k'^{15}_{\mathrm{d,L}}e^{-k'_{\mathrm{d}}15\Lambda} + w_{45}k'^{45}_{\mathrm{d,L}}e^{-k'_{\mathrm{d}}45\Lambda} + w_{75}k'^{75}_{\mathrm{d,L}}e^{-k'_{\mathrm{d}}75\Lambda}\right) \tag{66}$$

or in terms of effective extinction coefficients for diffuse radiation,

$$Q_{\mathrm{d,L}}(\Lambda) = (1-\alpha_{\mathrm{cd}})I_{\mathrm{d},0}k'_{\mathrm{d,L}}e^{-k'_{\mathrm{d}}\Lambda} \tag{67}$$

Equating these expressions gives:

$$k'_{\mathrm{d,L}} = \frac{w_{15}k'_{\mathrm{d,L}}15e^{-k'_{\mathrm{d}}15\Lambda} + w_{45}k'_{\mathrm{d,L}}45e^{-k'_{\mathrm{d}}45\Lambda} + w_{75}k'^{75}_{\mathrm{d,L}}e^{-k'_{\mathrm{d}}75\Lambda}}{e^{-k'_{\mathrm{d}}\Lambda}} \tag{68}$$

Similarly, the effective extinction coefficient for diffuse radiation for trunks is:

$$k'_{\mathrm{d,tr}} = \frac{w_{15}k'^{15}_{\mathrm{d,tr}}e^{-k'_{\mathrm{d}}15\Lambda} + w_{45}k'^{45}_{\mathrm{d,tr}}e^{-k'_{\mathrm{d}}45\Lambda} + w_{75}k'^{75}_{\mathrm{d,tr}}e^{-k'_{\mathrm{d}}75\Lambda}}{e^{-k'_{\mathrm{d}}\Lambda}} \tag{69}$$

A.3. Radiation sub-model: canopy reflection coefficients

In order to estimate canopy reflection coefficients for beam and diffuse radiation, we first require an estimate of the canopy reflection coefficient for theoretical horizontal canopy elements:

$$\alpha_{\mathrm{c,H}} = \frac{1-\tau_{\mathrm{L,tr}} - \sqrt{(1-\tau_{\mathrm{L,tr}})^2 - \alpha^2_{\mathrm{L,tr}}}}{\alpha_{\mathrm{L,tr}}} \tag{70}$$

Here $\tau_{L,tr}$ and $\alpha_{L,tr}$ are mean transmission and reflection coefficients for leaves and trunks, weighted by their projected areas on the ground, which vary depending on the relative amounts of incident direct and diffuse radiation:

$$\alpha_{\mathrm{L,tr}} = \frac{\alpha_{\mathrm{L}}w_{\mathrm{L}} + \alpha_{\mathrm{tr}}w_{\mathrm{tr}}}{w_{\mathrm{L}}+w_{\mathrm{tr}}} \tag{71}$$

$$\tau_{\mathrm{L,tr}} = \frac{\tau_{\mathrm{L}}+\tau_{\mathrm{tr}}}{w_{\mathrm{L}}+w_{\mathrm{tr}}} \tag{72}$$

where;

$$w_{\mathrm{L}} = \frac{Q_{\mathrm{d0}}w_{\mathrm{d,L}} + Q_{\mathrm{b0}}w_{\mathrm{b,L}}}{Q_{\mathrm{d0}}+Q_{\mathrm{b0}}} \tag{73}$$

$$w_{\mathrm{tr}} = \frac{Q_{\mathrm{d0}}w_{\mathrm{d,tr}} + Q_{\mathrm{b0}}w_{\mathrm{b,tr}}}{Q_{\mathrm{d0}}+Q_{\mathrm{b0}}} \tag{74}$$

and

$$w_{\mathrm{b,L}} = k_{\mathrm{b,L}}\Lambda_{\mathrm{L}} \tag{75}$$

$$w_{\mathrm{b,tr}} = k_{\mathrm{b,tr}}\Lambda_{\mathrm{tr}} \tag{76}$$

$$w_{\mathrm{d,L}} = \Lambda_{\mathrm{L}}(w_{15}k_{\mathrm{d,L}}^{15} + w_{45}k_{\mathrm{d,L}}^{45} + w_{75}k_{\mathrm{d,L}}^{75}) \tag{77}$$

$$w_{\mathrm{d,tr}} = \Lambda_{\mathrm{tr}}(w_{15}k_{\mathrm{d,tr}}^{15} + w_{45}k_{\mathrm{d,tr}}^{45} + w_{75}k_{\mathrm{d,tr}}^{75}) \tag{78}$$

The canopy reflection coefficients for beam and diffuse radiation are then given by:

$$\alpha_{\mathrm{cb}} = \frac{2k_{\mathrm{b}}}{k_{\mathrm{b}} + k_{\mathrm{d}}}\alpha_{\mathrm{c,H}} \tag{79}$$

$$\alpha_{\mathrm{cd}} = w_{15}\alpha_{\mathrm{c}}^{15} + w_{45}\alpha_{\mathrm{c}}^{45} + w_{75}\alpha_{\mathrm{c}}^{75} \tag{80}$$

where e.g.

$$\alpha_{\mathrm{c}}^{15} = \frac{2k_{\mathrm{d}}^{15}}{k_{\mathrm{d}}^{15} + k_{\mathrm{b}}^{15}}\alpha_{\mathrm{c,H}} \tag{81}$$

Finally, the effective soil–canopy reflection coefficients for beam and diffuse radiation are:

$$\alpha_{\mathrm{cb}}^{\mathrm{eff}} = \alpha_{\mathrm{cb}} + (\alpha_{\mathrm{s}} - \alpha_{\mathrm{cb}})e^{-2k_{\mathrm{b}}'\Lambda} \tag{82}$$

$$\alpha_{\mathrm{cb}}^{\mathrm{eff}} = \alpha_{\mathrm{cd}} + (\alpha_{\mathrm{soil}} - \alpha_{\mathrm{cd}})e^{-2k_{\mathrm{d}}'\Lambda} \tag{83}$$

where α_{soil} is the soil reflection coefficient.

References

Aston, A.R., 1985. Heat-storage in a young eucalypt forest. Agric. Forest Meteorology 35 (1–4), 281–297.

Blanken, P.D., Black, T.A., Yang, P.C., Neumann, H.H., Nesic, Z., Staebler, R., den Hartog, G., Novak, M.D., Lee, X., 1997. Energy balance and canopy conductance of a boreal aspen forest: partitioning overstory and understory components. J. Geophysical Res. Atmospheres 102 (D24), 28915–28927.

Chapman, A.J., 1984. Heat Transfer. Macmillan Publishing Company, New York, 608 pp.

Choudhury, B.J., Monteith, J.L., 1988. A four-layer model for the heat budget of homogeneous land surfaces. Q. J. R. Meteorological Soc. 114, 373–398.

Deardorff, J.W., 1978. Efficient prediction of ground surface-temperature and moisture, with inclusion of a layer of vegetation. J. Geophysical Res. Oceans Atmospheres 83 (NC4), 1889–1903.

Frumau, K.F.A., 1993. Aerodynamic Characteristics and Evapotranspiration from a Young Pinus Caribaea Plantation Forest near Tulasewa. Fiji, Vrije Universiteit, Amsterdam, 186 pp.

Goudriaan, J., van Laar, H.H., 1994. Modelling Potential Crop Growth Processes. Current Issues in Production Ecology 2. Kluwer Academic Publishers, Dordrecht, 238 pp.

Herrington, L.P., 1969. On temperature and heat flow in tree stems. Yale Univ. School Forestry Bull. 73, 22–40.

Jones, J.K., Webb, B.W., Jimenez, D., Reardon, J., Butler, B., 2004. Development of an advanced one-dimensional stem heating model for application in surface fires. Can. J. Forest Res. 34 (1), 20–30.

Lamaud, E., Ogee, J., Brunet, Y., Berbigier, P., 2001. Validation of Eddy flux measurements above the understorey of a pine forest. Agric. Forest Meteorology 106, 187–203.

Leuning, R., Cleugh, H.A., Zegelin, S.J., Hughes, D., 2005. Carbon and water fluxes over a temperate Eucalyptus forest and a tropical wet/dry savanna in Australia: measurements and comparison with MODIS remote sensing estimates. Agric. Forest Meteorology 129 (3–4), 151–173.

Leuning, R., Kelliher, F.M., Depury, D.G.G., Schulze, E.D., 1995. Leaf nitrogen, photosynthesis conductance and transpiration—scaling from leaves to canopies. Plant Cell Environ. 18 (10), 1183–1200.

Lin, J.D., 1980. On the Force-Restore method for prediction of ground surface temperature. J. Geophysical Res. 85, 3251–3254.

McCaughey, J.H., Saxton, W.L., 1988. Energy-balance storage terms in a mixed forest. Agric. Forest Meteorology 44 (1), 1–18.

Meesters, A., Vugts, H.F., 1996. Calculation of heat storage in stems. Agric. Forest Meteorology 78 (3–4), 181–202.

Monteith, J.L., Unsworth, M., 1990. Principles of Environmental Physics. Edward Arnold, London, 291 pp.

Moore, C.J., Fisch, G., 1986. Estimating heat-storage in amazonian tropical forest. Agric. Forest Meteorology 38 (1–3), 147–168.

Oliphant, A.J., Grimmond, S.B., Zutter, H.N., Schmid, H.P., Su, H.B., Scott, S.L., Offerle, B., Randolph, J.C., Ehman, J., 2004. Heat storage and energy balance fluxes for a temperate deciduous forest. Agric. Forest Meteorology 126 (3–4), 185–201.

Potter, B.E., Andresen, J.A., 2002. A finite-difference model of temperatures and heat flow within a tree stem. Can. J. Forest Res.-Revue Canadienne De Recherche Forestiere 32 (3), 548–555.

Raupach, M.R., 1989. A practical Lagrangian method for relating scalar concentrations to source distributions in vegetation canopies. Q. J. R. Meteorological Soc. 115 (487), 609–632.

Ross, J., 1981. The Radiation Regime and Architecture of Plant Stands. Tasks for Vegetation Sciences. Dr W. Junk Publishers, The Hague, 391 pp.

Sellers, P.J., 1985. Canopy reflectance, photosynthesis and transpiration. Int. J. Remote Sensing 6, 1335–1372.

Silberstein, R., Held, A., Hatton, T., Viney, N., Sivapalan, M., 2001. Energy balance of a natural jarrah (Eucalyptus marginata) forest in Western Australia: measurements during the spring and summer. Agric. Forest Meteorology 109 (2), 79–104.

Silberstein, R.P., Sivapalan, M., Viney, N.R., Held, A., Hatton, T.J., 2003. Modelling the energy balance of a natural jarrah (Eucalyptus marginata) forest. Agric. Forest Meteorology 115 (3–4), 203–232.

Simpson, W. TenWolde, A., 1999. Physical properties and moisture relations of wood Wood handbook- wood as an engineering material. USDA Forestry Service General Techinical Report.

Sokal, R.R., Rohlf, F.J., 1995. Biometry. W.H. Freeman and Company, New York, 887 pp.

Thom, A.S., 1975. Momentum, heat and mass exchange of plant communities. In: Monteith, J.L. (Ed.), Vegetation and the Atmosphere. Academic Press, London, pp. 57–109.

Wang, Y.P., Leuning, R., 1998. A two-leaf model for canopy conductance, photosynthesis and partitioning of available energy I: Model description and comparison with a multi-layered model. Agric. Forest Meteorology 91 (1–2), 89–111.

Wilson, K., Goldstein, A., Falge, E., Aubinet, M., Baldocchi, D., Berbigier, P., Bernhofer, C., Ceulemans, R., Dolman, H., Field, C., Grelle, A., Ibrom, A., Law, B.E., Kowalski, A., Meyers, T., Moncrieff, J., Monson, R., Oechel, W., Tenhunen, J., Valentini, R., Verma, S., 2002. Energy balance closure at FLUXNET sites. Agric. Forest Meteorology 113 (1–4), 223–243.